Materials Science and Engineering B 296 (2023) 116710

Contents lists available at ScienceDirect

Materials Science & Engineering B

journal homepage: www.elsevier.com/locate/mseb

Theoretical development of the CZTS thin-film solar cell by SCAPS-1D software based on experimental work

Abdelaziz Ait Abdelkadir *, Mustapha Sahal *

MESE/Lab.PETI, Ouarzazate Polydisciplinary Faculty, University of Ibn Zohr, Morocco

ARTICLE INFO

Keywords:
Solar cell
CZTS
MoO_x B.S.F
22.28% efficiency

ABSTRACT

In this work, the SCAPS-1D program was used to develop and simulate Al-ZnO/CdS/CZTS/MoS_2/Mo conventional solar cell structure. We enhanced numerous parameters, including CZTS thickness, MoS_2 interlayer thickness, and carrier concentration, after device validation using experimental results. With a V_{oc} of 0.81 V, J_{sc} of 16.83 mA/cm^2, and FF of 65.84 %, the highest experimental efficiency is 8.98%. However, we found that low efficiency is caused by defect density and the formation of MoS_2 interlayers, both of which are generated by high recombination. In order to minimize this recombination, we proposed employing MoO_x as the back-surface field and "Au" as the bottom contact. After device adjustment, a high performance of 22.28 % was achieved employing 20 nm of MoO_x and a CZTS defect concentration of 10^{13} cm^{-3} in the new Al-ZnO/CdS/CZTS/MoO_x/Au solar cell.

1. Introduction

In recent years, interest in CZTS quaternary compound semiconductors has grown significantly, owing to their strong similarities to the well-studied high-efficiency copper indium gallium selenide (CIGS), which has an ideal band gap of 1.5 eV and an absorption coefficient higher than 10^4 cm^{-1} [1]. Each CZTS constituent is abundant in the earth's crust (Cu: 50 ppm, Zn: 75 ppm, Sn: 2.2 ppm, S: 260 ppm) and has very low toxicity [2] when compared to CIGS, which have rare and expensive compounds like In and Ga, making CZTS superior to CIGS [3]. The melting point temperature range of the CZTS compound, on the other hand, is 1260 K, making the composite more suitable for very high-temperature synthesis [4]. The CZTS-based thin film absorber is fabricated through different physical and chemical-based approaches, including sputtering [5], electron beam deposition [6], and electrochemical deposition [7] (see Table 1).

According to the Shockley-Queisser limit, a solar cell with a band gap of 1.5 eV (CZTS) can achieve an optimum conversion efficiency of roughly 32.2% [8,9]. In an experiment conducted in 2008, the sulfurization approach was used to boost CZTS efficiency to 6.7% [3]. In 2013, the efficiency of CZTS-based thin-film photovoltaic power conversion exceeded 8.4% [10].

Double-pressure sputtering was used in 2021 to create an ultra-thin CZTS thin film solar cell with a high efficiency of 9.3% using a single quaternary compound target that had been created by spark plasma sintering [11]. In order to achieve a high Cu_2CdSnS_4 thin film quality with a 10% efficiency, FAN et al. highlight the significance of utilizing optimum sulfurization and optimizing ratios (Cu/Cd + Sn) and temperatures [12]. In 2022, Ye Chen et al. showed that dual-cation (Ag and Ti) substituted CZTSSe can hence increase power conversion to 12.73% [13]. The limitation of the efficiency of CZTS-based thin-film solar cells is attributed to their poor open-circuit voltage and fill factor, which are mainly caused by antisite defects and an unfavorable heterojunction interface [14]. Recently, a thick MoS_2 layer was observed to increase the device resistance while degrading V_{oc} [15,16]. By introducing WO_3 as a back surface field, ZHAO et al. demonstrated the possibility of solving the traditional problems of phase segregation, voids in the absorber, and overly thick Mo(S, Se)$_2$ at the back interface between the back electrode and CZTSSe absorber layer, increasing the efficiency to 12.66% [17]. To increase the commercial viability of CZTS solar cells and improve their efficiency to that of CIGS solar cells, major challenges must be addressed, such as interfaces between CZTS/Mo and CdS/CZTS, as well as minimizing defect concentration, because the efficiency of CZTS-based solar cells is dependent on open-circuit voltage (V_{oc}), current density (J_{sc}), and fill factor (FF). Carrier generation and recombination at the interfaces boost V_{oc} in solar cells. As a result, the CdS/CZTS solar cell's conversion efficiency is exceedingly poor. As a result, some scientists claim that MoS_2 hurts solar cell devices [18,19].

* Corresponding authors.
E-mail addresses: abdelazizaitabdelkadir@gmail.com (A. Ait Abdelkadir), sahalmustapha@gmail.com (M. Sahal).

https://doi.org/10.1016/j.mseb.2023.116710
Received 23 March 2022; Received in revised form 9 June 2023; Accepted 2 July 2023
Available online 5 July 2023

Table 1
Back and front contacts parameters.

Parameters	Front contact	Back contact
Metal work function $\varphi(eV)$	Flat	4.63–5.6 eV
$S_e(cm\bullet S^{-1})$	10^7	10^7
$S_h(cm\bullet S^{-1})$	10^7	10^7

In this study, we examine the influence of CZTS and MoS_2 thicknesses, charge carrier concentration, and bottom metal contact on the CZTS-based solar cell characteristics following theoretical validation of the Al-ZnO/CdS/CZTS/MoS_2/Mo solar cell with experimental work using SCAPS-1D software. Moreover, we investigated the impact of the insertion of MoO_x HTL as an intermediate layer between CZTS/Metal contact and the bottom metal work function on solar cell efficiency. We explored the influence of parasitic resistance on the novel solar cell characteristics in particular, and the various optimized findings were compared to existing theoretical and practical studies. Based on the various experimental impacts, maximum efficiency of 22.28% was recorded from the Al-ZnO/CdS/CZTS/MoO_x/Au new solar cell.

2. Material parameters and device architecture

SCAPS-1D is an excellent tool for simulating the performance of solar cells developed by the University of Gent and can provide a good agreement between experiment and simulation results [20]. SCAPS-1D software is utilized in this study to extract experimental CZTS solar cell properties using a curve fit model. SCAPS-1D is based on the theoretical computation and resolution of three basic equations: Poisson's equation (1), hole continuity and electron continuity equations (2–3), and drift–diffusion (4–5) at each position throughout the device, taking into account the boundary conditions.

$$\frac{d^2}{dx^2}\psi(x) = \frac{e}{\varepsilon_0\varepsilon_r}(p(x) - n(x) + N_D - N_A + \rho_P - \rho_n) \quad (1)$$

$$-\frac{\partial j_n}{\partial x} - U_n + G = \frac{\partial n}{\partial t} \quad (2)$$

$$-\frac{\partial j_p}{\partial x} - U_p + G = \frac{\partial p}{\partial t} \quad (3)$$

$$j_n = -\frac{U_n n}{q}\frac{\partial E_{Fn}}{\partial x} \quad (4)$$

$$j_p = -\frac{U_p p}{q}\frac{\partial E_{Fp}}{\partial x} \quad (5)$$

where $\psi(x)$ is the electrostatic potential, e is an electrical charge, ε_0 and ε_r are the relative and vacuum permittivity, p and n are hole and electron concentrations, N_D and N_A are donor and acceptor charge impurities, ρ_p and ρ_n are hole and electron distributions, respectively. G represents the generation rate, whereas j_n and j_p represent the electron-hole current densities. The Poisson and continuity equations provide a set of coupled differential equations (Ψ, n, p) or (Ψ, E_{Fn}, E_{Fp}) with appropriate boundary conditions at interfaces and contacts. Fig. 1 summarizes the conventional and optimum solar cell configurations studied in this work, as well as the associated band diagram obtained using SCAPS-1D software.

3. Results and discussion

3.1. Validation of CZTS simulated parameters with experimental work

Firstly, the available experimental parameters of the CZTS based solar cell, such as layer thickness, carrier concentration, MoS_2 thickness, R_s, and R_{sh}, were collected from Tara P. Dhakal [24] experimental work,

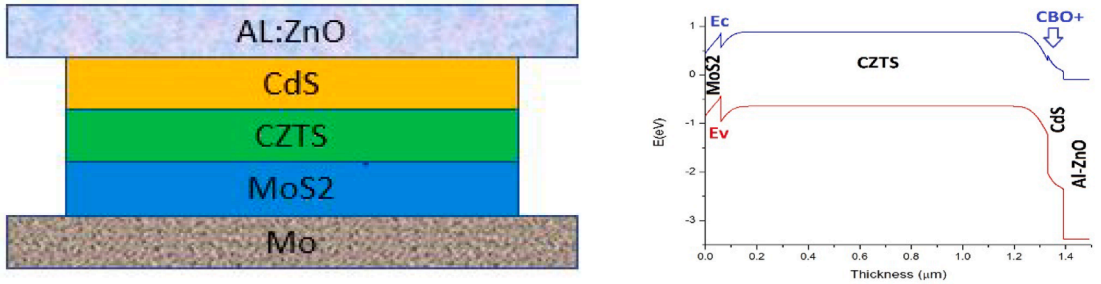

a) Conventional configeration

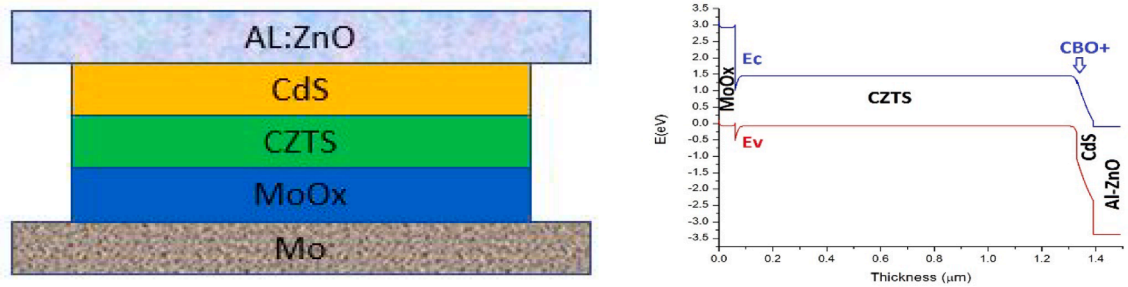

b) Optimal configuration

Fig. 1. The two configurations of analyzed solar cells in this work.

as well as Tables 2, 3, and 4. These parameters were integrated into the SCAPS-1D software after starting the test in order to know the origin of the poor efficiency of the CZTS-based solar cell. Fig. 2 depicts both the theoretical and experimental J-V curves. We notice that, at 9.10^{14} cm^{-3} in CZTS defect density, we found a strong agreement between the experimental and theoretical J-V curves, highlighting that the SCAPS −1D program is an excellent tool for describing the development of CZTS-based solar cells. We got a J_{SC} of 18.14 mA/cm^2, a V_{OC} of 0.62 V, a FF of 54.40%, and a power conversion efficiency (PCE) of 6.16%, which is in good consensus with experimental values reported by Dhakal (**see** Table 4).

3.2. Effect of CZTS and MoS_2 thickness on the conventional solar cell characteristics.

As known, absorber layer characteristics such as thickness and carrier concentration play a key role in enhancing solar cell efficiency because a thin absorber layer results in inefficient light absorption and a thick absorber layer leads in recombination current in the bulk. So, the absorber layer is one of the great parameters that limit the performance of solar cells.

In this section, a simple structure (Al-ZnO/CdS/CZTS/MoS_2/Mo) for the baseline case of the CZTS cell (See Fig. 1) was chosen as the starting point of this analysis. As shown in Fig. 3 **a**, a numerical simulation was done using SCAPS-1D software by varying the CZTS thickness from 0.2 μm to 2 μm whereas other physical parameters were kept constant. We found that the solar cells' efficiency (PCE) increases as the CZTS absorber layer increased due to the enhancement in photo-generated current with the thickness (absorb the long-wavelength photon as shown in Fig. 3**.a** and **b**). A thickness greater than ~ 1300 nm, a small increase in efficiency, and a large decrease in FF were observed, which can be attributed to Auger recombination [26], bimolecular recombination [27], and Shockley-Read-Hall (SRH) recombination [28,29]. That greatly contributed to increasing the device's total recombination and series resistance due to the high density of defects on the CZTS absorber layer ($9.10^{14}cm^{-3}$). At ~ 1300 nm thickness, the optimal efficiency of 6.16 %, V_{oc} of 0.62 V, J_{sc} of 18.4 mA/cm^2, and FF of 54.4 % are found, which is similar to the thickness employed experimentally by Dhakal [24]. Hence, we investigated the thickness impact of MoS_2 formed at back contact between CZTS and Mo in the 20–300 nm range, as shown in Fig. 4. We revealed that MoS_2 formed to act as B.S.F for CZTS, increasing efficiency, but only for a very small thickness of < 40 nm, and for a thickness greater than 40 nm, a massive decrease in photocurrent was observed, which can be contributed to the recombined of photo-generated electron-hole pairs in the CZTS/Mo interface without reaching the rear contact region. some papers have explained that these layers affect the open circuit voltage due to the shifting band alignment between CZTS and Mo interfaces [30–32].

Table 2
Optimized materials proprieties used in the simulation.

Parameters	MoO_x [21]	MoS_2 [22]	CZTS [23,24]	CdS [25]	Al-ZnO [23]
Thickness (nm)	20	40	1270	50	100
E_g (eV)	3.2	1.29	1.53	2.42	3.33
χ(eV)	2.3	4.2	4.5	4.4	4.55
ε_r	10	4	9.5	10	8.12
$N_C\,(cm^{-3})$	$3.2.10^{16}$	$7.5.10^{17}$	$1.91.10^{18}$	$1.2.10^{18}$	$4.1.10^{18}$
$N_V\,(cm^{-3})$	$2.5.10^{17}$	$1.8.10^{18}$	$2.58.10^{18}$	$1.8.10^{19}$	$8.2.10^{18}$
μ_N(cm^2/v.s)	30	100	50	100	100
μ_P(cm^2/v.s)	2.5	150	100	50	20
$N_D(cm^{-3})$	0	0	0	$2.1.10^{17}$	10^{20}
$N_A(cm^{-3})$	5.10^{17}	1.10^{21}	$5.65.10^{16}$	0	0

where E_g is the band gap, χ the electron affinity, ε dielectric permittivity, N_C, states density of the conduction band, N_V states density of the valence band, V_{thn} electron thermal velocity, V_{thp} hole thermal velocity, μ_n electron mobility, μ_p hole mobility, N_A donor density, and N_D acceptor density. The absorption coefficient of all layers was taken from the literature.

Table 3
Interface parameters used in the Al-ZnO/CdS/CZTSe/Mo heterojunction device simulation and defect density parameters of employed materials.

Parameter	CdS/CIGS	CZTS/MoO_x
Defect type	Neutral	Neutral
Capture cross section electrons	10^{-19}	10^{-19}
Capture cross-section holes	10^{-19}	10^{-19}
Reference for defect energy level E_t	above the highest Ev	
Energy with respect to Reference (eV)	0.06	0.06
Total density	10^{10}	10^{10}

Defects properties	Al-ZnO	CdS	CZTS	MoO_x
Defects density N_t (cm^{-3})	A:10^{17}	$A : 10^{17}$	$D : 9.10^{14}$	$D : 10^{14}$
$\sigma_n(cm^2)$	10^{-12}	10^{-17}	2.10^{-14}	2.10^{-14}
$\sigma_p(cm^2)$	10^{-15}	10^{-13}	2.10^{-14}	2.10^{-14}
$E_A or E_D$(eV)	Medium of the gap			
Defect type	Single Acceptor		Single Donor	Neutral
Energetic distribution	Single	GauB	Single	Single
Reference for defect energy level Et	Above EV (SCAPS<2.7)			
Energy level with respect to reference BV	0.6	0.1	0.6	0.6

Table 4
Validation of CZTS S.C. parameters for studied structures.

Absorber layer	Ref	Photovoltaic parameters			
		J_{SC} (mA/cm^2)	V_{OC} (V)	FF (%)	η (%)
CdS/CZTS	This work	19	0.60	55	6.2
CdS/CZTS	Experimental [24]	18.14	0.62	54.40	6.16

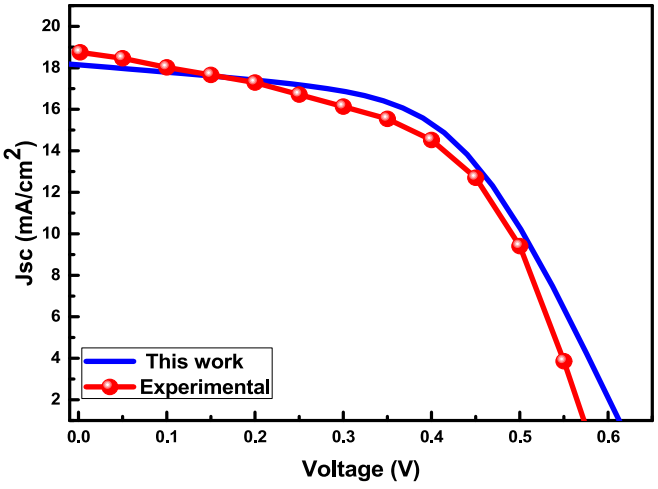

Fig. 2. Comparing J-V characteristics of experimental [24] and simulated conventional solar cell structures (Fig. 1-a).

3.3. Effect of the carrier concentration of CZTS and MoS_2 layers on the conventional solar cell characteristics.

In this section, we investigated the effects of CZTS and MoS_2 layer carrier concentrations on CZTS solar cell characteristics under the sum modulated condition gated, taking into consideration the experimental parasitic resistance reported in the literature [24]. Greatest efficiency of 8.98%, V_{oc} of 0.81 V, J_{sc} of 16.83 mA/cm^2, and FF of 65.46 % are got at 5.75. 10^{17} cm^{-3} and 10^{18} cm^{-3} in carrier concentration of CZTS and

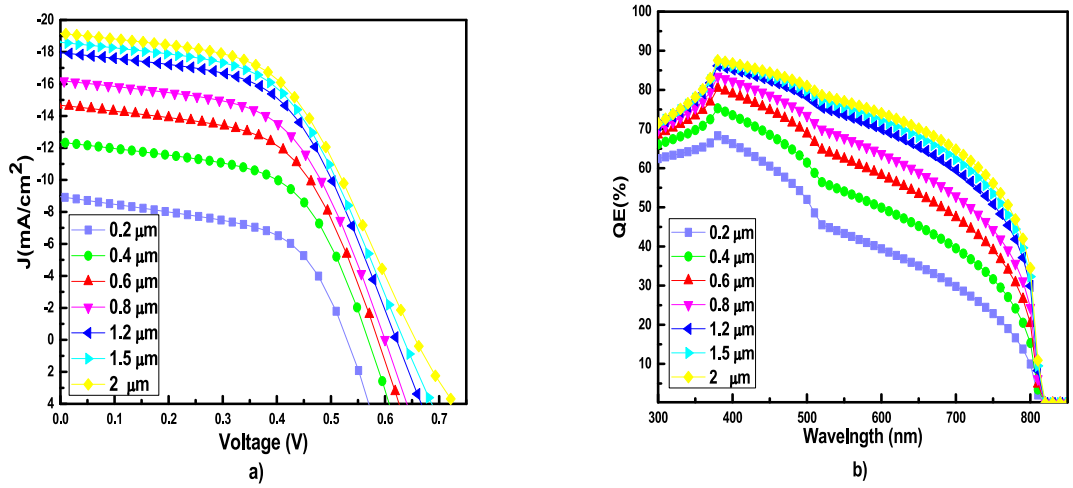

Fig. 3. Effect of CZTS thickness on QE and J-V of the conventional solar cells.

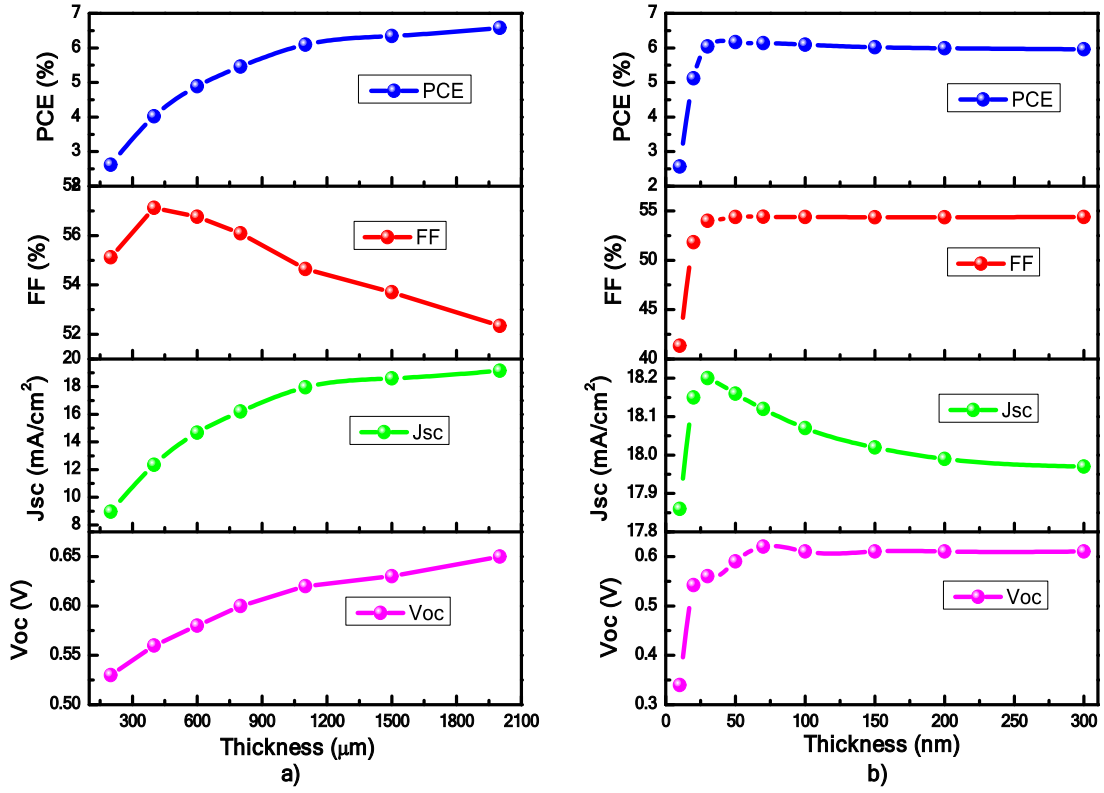

Fig. 4. Impact of CZTS (a) and MoS_2 (b) thickness on the PV characteristics of studied heterostructure.

MoS_2 respectively, which nearly agrees with the maximum efficiency reported in the literature for CZTS [10] (See Fig. 5 and Table 5).

The little difference can be attributed to the differences in defect concentration, thickness, and E_g. Finally, we can see that two interesting features are the original causes of the low efficiency of the CZTS based solar cell, which are high defect carrier concentration ($\sim 9.10^{14}$ cm^{-3}) and the type of interfaces formed with the bottom metal work function (Mo) which is also the origin of the high resistance. In the next section, we proposed employing the MoO_x hole transport layer as the back-surface field, "Au" as bottom contact to ameliorate the CZTS solar cell efficiency. We will be also analyzing the effect of CZTS defect density and parasitic resistance on CZTS solar cell performance.

3.4. Effect of the incorporation of MoO_x and bottom metal work function on CZTS solar cell characteristics.

The effect of MoO_x/Au on quantum efficiency and light (J-V) measurements for solar cells based on CZTS thin films is depicted in Fig. 6. We can observe that the PCE increases from 8.98% for the CZTS solar cell with MoS_2 to 9.90% for the same solar cell but with MoO_x, indicating that the MoO_x reflector layer improves the V_{oc} which enhances the CZTS-based solar cell efficiency.

Fig. 7 displays the new solar cell's photovoltaic performance in regard to MoO_x layer thickness and metal work function. The MoO_x thickness varied from 20 nm to 100 nm. From this figure, we can notice the invariance of the J_{sc} and V_{oc} with MoO_x layer thickness, which can be attributed to the high work function of MoO_x HTL, revealing that a thin

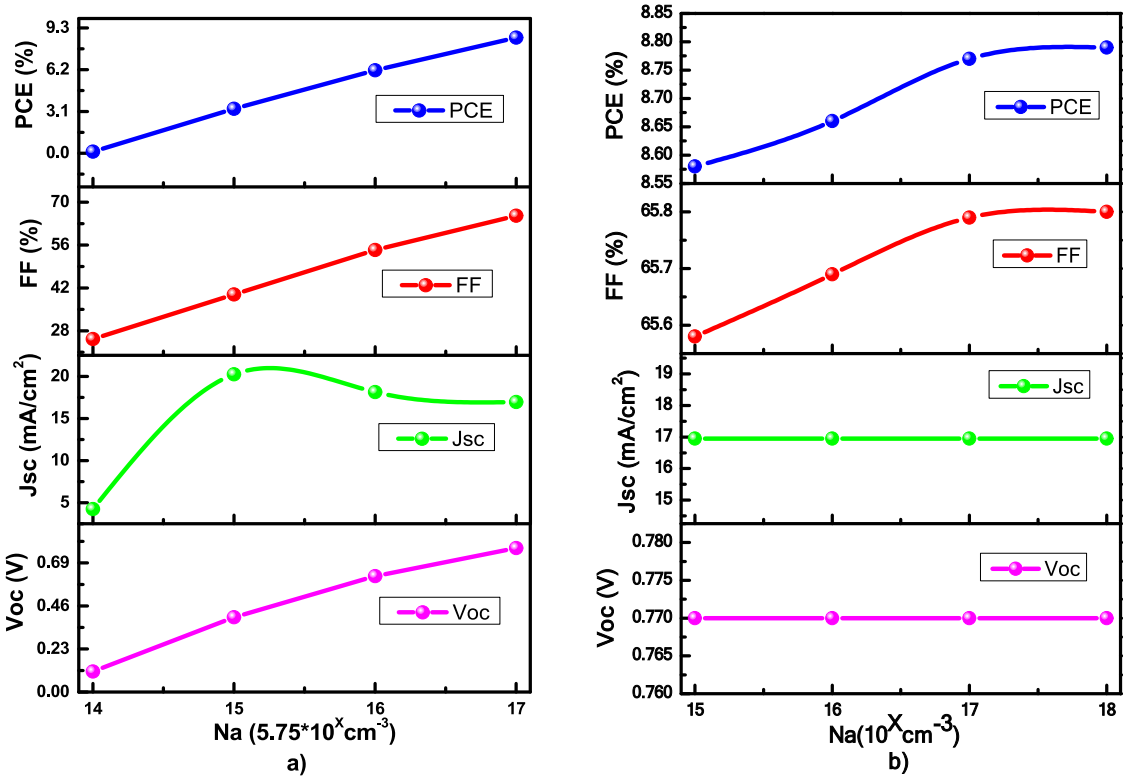

Fig. 5. The effect of CZTS (a) and MoS_2 (b) carrier concentration on conventional solar cells characteristics.

Table 5
The maximum efficiency obtained for Al-ZnO/CdS/CZTS/MoS_2/Mo.

Absorber layer	Ref	Photovoltaic parameters			
		J_{SC} (mA/cm²)	V_{OC} (V)	FF (%)	η (%)
CdS/CZTS(E_g = 1.53ev)CdS/CZTS (E_g = 1.45ev)	This work	16.83	0.81	65.46	8.98
	Experimental [10]	19.5	0.66	65.80	8.4

layer of MoO_x HTL can generate a high built potential to reflect electrons from back contact to the n-type side. A similar effect has been reported in the literature for several HTL in various solar cells based on thin films such as CZTSe, CZTGS, Sb_2Se_3 and CIGS [28,29,33,34]. Furthermore, owing to the advantageous conduction and valence band offset between the absorber layer and the BSF layer, MoO_x BSF provides a highly conductive path for holes to easily separate and transport from the CZTS absorber layer to the output terminal.

However, the effect of the bottom metalwork function on the Al-ZnO/CdS/CZTS/MoO_x/Metal hetero solar cell was analyzed and shown in Fig. 7**.b.** As the work function of the back-contact increases, the four parameters that determine the yield of the studied S.C. device also increase. That can be explained by the decrease in the height barrier on the valence band as a result of the easier movement of the photogenerated holes in the quasi-neutral region (QNR) from the CZTS to the back contact, which improves the V_{oc} and the performance of the CZTS based solar cell (See Fig. 6**.b**). Therefore, hole recombination with input electrons from the external circuit is done at a higher rate, and this

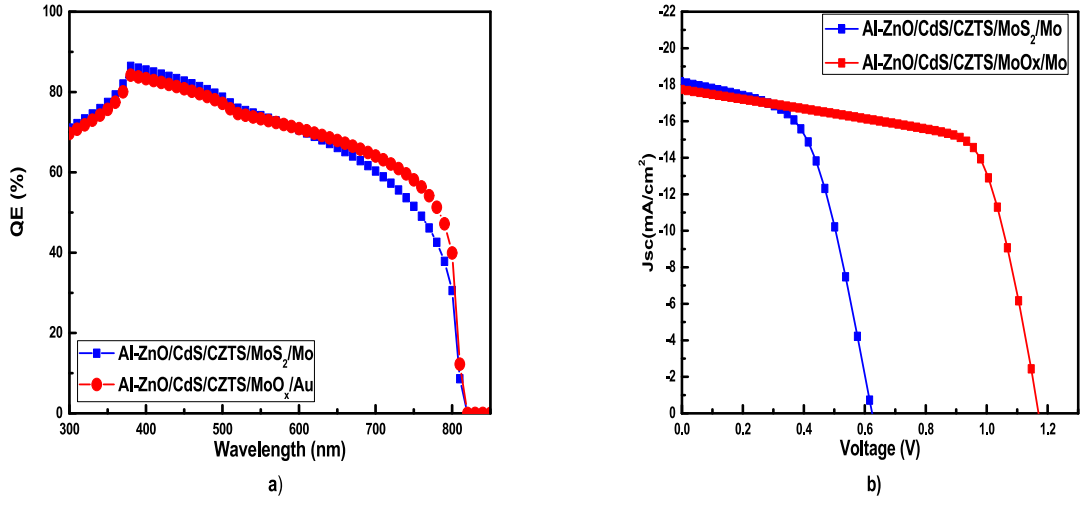

Fig. 6. Effect of MoO_x/Au on the Quantum efficiency (EQE) and light (J-V) measurements for CZTS based solar cell.

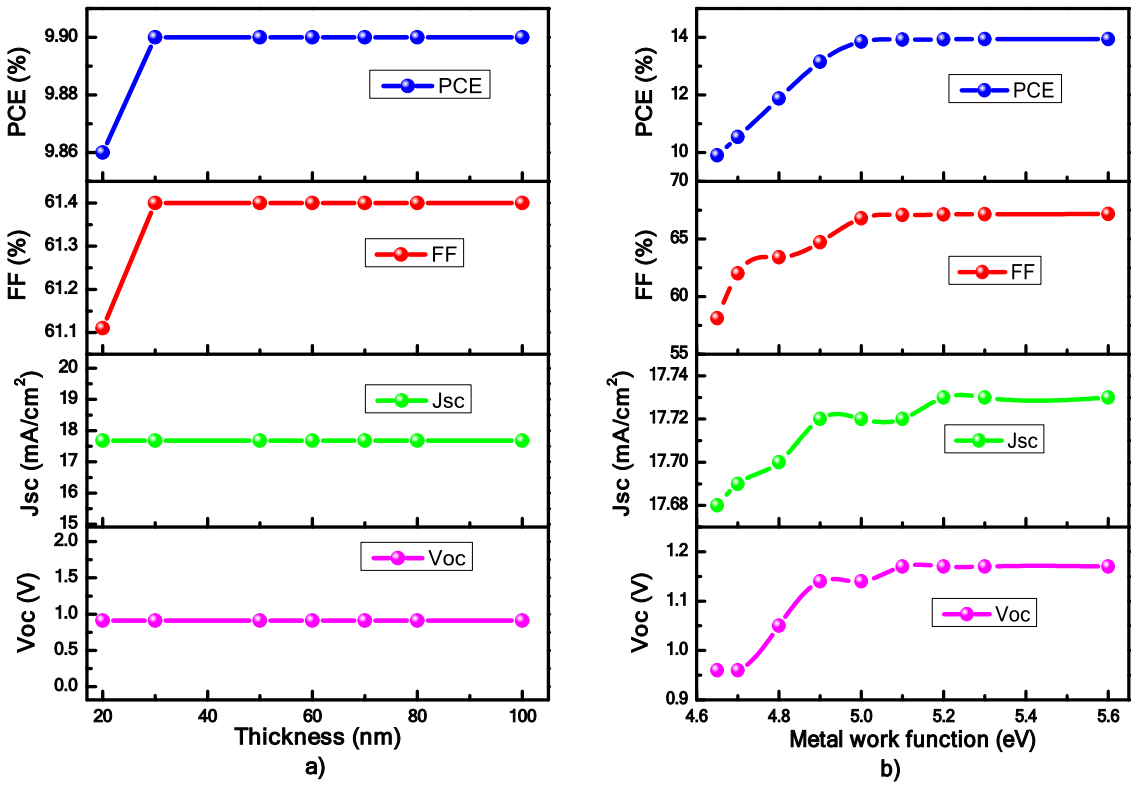

Fig. 7. Effect of MoO_x HTL interlayer thickness (a) and metals work function (b) on the new solar cell characteristics (Fig. 1. b).

enhances open-circuit voltage and efficiency. The optimum PCE, FF, J_{sc}, and V_{oc} of 13.94%, 67.16%, 17.73 mA/cm^2, and 1.17 V respectively, were obtained at 5.1 eV on the metalwork function, which corresponds to the "Au" metalwork function.

3.5. Effect of CZTS defect density and parasitic resistance on new hetero solar cell characteristics

As indicated in the previous section, CZTS compounds have a high defect density (9.10^{14} cm^{-3}), limiting the efficiency of the Al-ZnO/CdS/CZTS/MoO_x/Au solar cell to 13.93%. Bin Liu et al. [35] used Na doping to increase the possibility of suppressing harmful antisite defects in CZTS Kesterite materials. Na doping improves the band alignment of the absorber/buffer interface and inhibits SRH recombination via the Na passivation effect, as well as the suppression of Sn_{Zn} defects, which is critical for increasing the CZTS solar cells efficiency. A similar result was observed when Ag or Mn was used to dope CZTS (Se) compounds [36,37]. However, improvements in CZTS crystal quality and device performance based on K surfactant are consistent with early theories and experimental observations work [38]. For this reason, in this part, we investigated the studied cell performance as a function of CZTS defect density in the range of 10^{13}–5.10^{15} cm^{-3}, as shown in Table 6. As regarding the defect density, current density, V_{oc}, and FF are degraded excessively with the increase of defect density, which could be due to the increase in trap-assisted carrier recombination and the SRH process. The PCE was drastically reduced from 22.28 to 9.81% with an increase in CZTS defect density from 10^{13} to 5.10^{15} cm^{-3}.

Table 6
The impact of CZTS defect density on the new solar cell efficiency studied in this work.

Defect density	Photovoltaic parameters			
	J_{sc} (mA/cm^2)	V_{oc} (V)	FF (%)	η (%)
1.10^{13} (cm^{-3})	24.81	1.29	71.01	22.28
5.10^{13}(cm^{-3})	23.99	1.24	69.98	20.96
1.10^{14}(cm^{-3})	23.10	1.22	69.57	19.77
5.10^{14}(cm^{-3})	19.29	1.18	68.08	15.57
1.10^{15}(cm^{-3})	17.46	1.16	67.01	13.67
5.10^{15}(cm^{-3})	13.53	1.11	64.82	9.81

3.6. Effect of parasitic resistance on new CZTS hetero solar cell characteristics

It is highlighted that the reduction in recombination at back contact caused by low defect density and a good collection of charge on CZTS-based solar cells well decreased significantly their resistance. As we know, parasitic resistance has a major impact on the CZTS solar cells' performance. However, SCAPS-1D software was employed to perform a numerical simulation to analyze the effect of parasitic resistance on the Al-ZnO/CdS/CZTS/MoO_x/Mo solar cells performance with a CZTS defect density of 10^{13} cm^{-3}. As illustrated in Fig. 8, the R_s and R_{sh} are adjusted in the 0–10 Ω.cm^2 and 200–1400 Ω.cm^2 ranges, respectively. It is observed that at lower series resistance (R_s < 5.1 Ω.cm^2) and high shunt resistance (R_{sh} > 400 Ω.cm^2), results in a better efficiency with a higher FF and J_{sc}. Furthermore, taking into consideration the available experimental parasitic resistance in the literature [24], we found an efficiency of 22.28 %. Table 7 illustrates a comparison of results obtained in this study with those found in the literature.

As shown in Table 7, after device validation of the CZTS conventional solar cell with experimental result [20], with an efficiency of 6.16 %, we found that there are several causes for the poor efficiency of the CZTS dispositive, such as low carrier concentration, high defect density, and the formation of MoS_2 interfaces. Following that we start optimizing solar cell thickness and carrier concentration to enhance the CZTS S.C. yield. In this study, we keep the E_g at 1.53 eV, R_s at 5.76 Ω.cm^2, and R_{sh} at 400 Ω.cm^2 similar to the experimental results reported in the literature [20]. An efficiency of 8.98 % (**optimized-1**) was obtained by adjusting the CZTS and MoS_2 thicknesses at 1300 nm and 40 nm, CZTS, and MoS_2 carrier concentrations of 5.75x10^{17} cm^{-3} and 10^{18} cm^{-3} respectively, that is in excellent accord with the finding in the literature

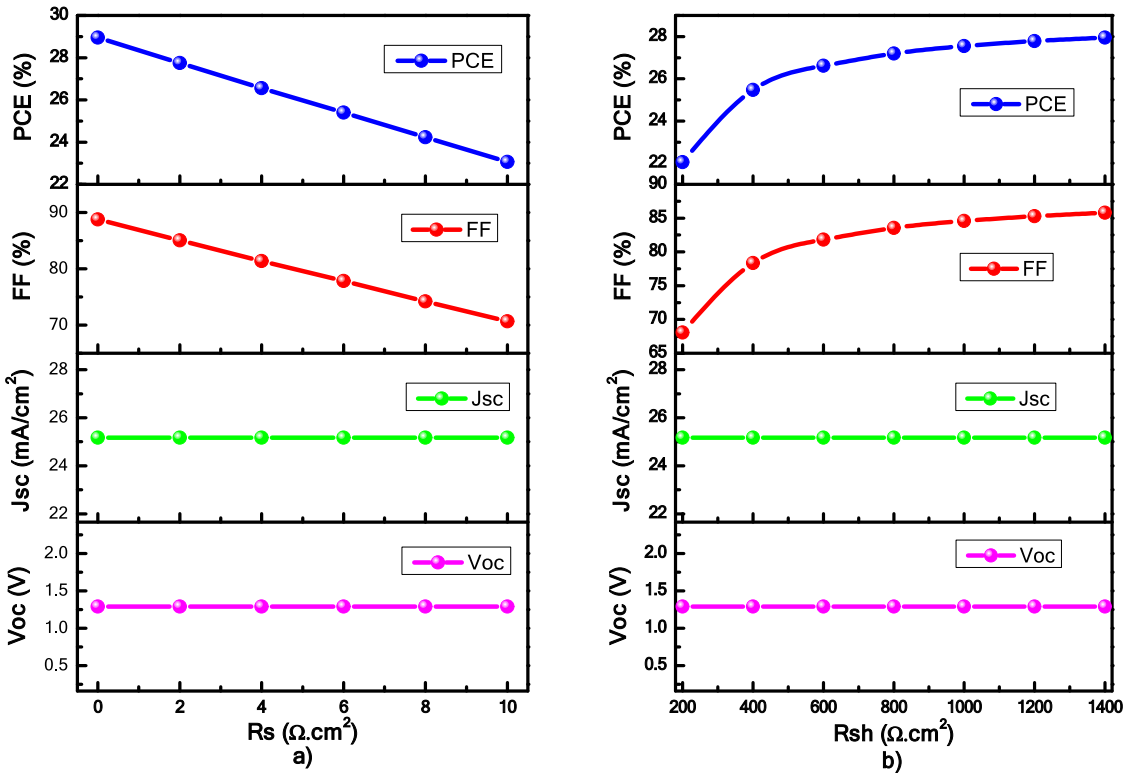

Fig. 8. Effect of R_s resistance (a), and R_{sh} resistance (b) on Al-ZnO/CdS/ CZTS/ MoO_x/Mo hetero solar cell characteristics.

Table 7
A comparison study between the results of this work with those found in the literature.

Structure	Type	E_g (eV)	R_s (Ω. cm^2)	R_{sh} (Ω. cm^2)	Defect (cm^{-3})	η (%)
CdS/CZTS/ MoS_2/Mo (4.65 eV)	**Validation**	1.53	5.76	400	**$9x10^{14}$**	6.16
	Experimental [24]	1.53	5.76	400	Unknown	6.2
	Optimized −1	1.53	5.76	400	**$9x10^{14}$**	8.98
CdS/CZTS/ MoS_2/Mo (4.65 eV)	**Optimized-2**	1.53	5.76	400	**$9x10^{14}$**	9.90
CdS/CZTS/ **MoS_2**/Mo (4.65 eV)	**Optimized-3** [39]	-	1.97	-		8.75
CdS/CZTS/ **MoO_x**/Mo (4.65 eV)	**Optimized-4** [20401]	1.53	5.76	400	**$9x10^{14}$**	13.94
CdS/CZTS/ Al_2O_3/Mo		1.5	-	-	$5x10^{14}$	12.43
CdS/CZTS/ **MoO_x/Au** (5.1 eV)		1.5	4.25	370	–	12.03
CdS/CZTS/ Au (5.1ev)		1.45	-	-	10^{15}	11.34
CdS/CZTS/ M (5ev)		1.53	5.76	400	**10^{13}**	22.28
CdS/CZTS/ Mo						
CdS/CZTS/ MoO_x/Au (5.1 eV)						

[29]. Flowing that, in order to eliminate the formation of the MoS_2 interlayer, we substitute the MoS_2 interlayer with MoO_x (**optimized-2**) to study the impact of BSF type on CZTS S.C. performance. High efficiency of 9.90 % was achieved, which means that MoO_x can greatly reduce back contact recombination compared to MoS_2 due to their high CBO. After this step, we investigated the influence of work function bottom metal contact on the Al-ZnO/CdS/CZTS/MoOx/Metal yield. We found that it is possible to increase the efficiency to 13.94 % using bottom contacts with metal work functions greater than 5.1 eV like Au, Ni, and Pt (**optimized–3**). Finally, an efficiency of 22.28 % was achieved by decreasing the CZTS density of defect from 10^{14} cm^{-3} to 10^{13} cm^{-3} (**optimized –4**). The reliability and accuracy of our method will inspire researchers to do experiments for enhancing CZTS S.C. with a similar configuration studied in this work.

4. Conclusion

SCAPS-1D software is utilized in this research to examine the yield of solar cells based on CZTS thin-film, an abundant non-toxic material, using experimentally available parameters. The practical and theoretical results agreed very well, which increases the possibility of describing CZTS-based solar cell properties through SCAPS-1D. The PCE was found to rise with the width of the CZTS absorber film and the concentration of carrier charges. However, we observed that a thinner layer of MoS_2 acts as a back-surface field, whereas a large thick of MoS_2 lowers solar cell performance due to high recombination and poor alignment of CZTS and MoS_2. Furthermore, we proved that MoO_x is a potential hole transport material with an "Au" bottom contact that has the potential to ameliorate the CZTS-based solar cell's performance. The greatest PCE of 22.28 % was found with CZTS thick, charge concentration, and defect density of 1300 nm, 10^{18} cm^{-3}, and 10^{13} cm^{-3}, respectively. The thickness of MoO_x, the density of CZTS deep level defects, and parasitic resistance were also investigated. The solar cell with the highest performance has a CZTS defect density of 10^{13} cm^{-3}, $R_s < 5.76$ Ω.cm^2 and $R_{sh} > 400$ Ω.cm^2. As a result, this research can offer the needed procedures for the applied design and enhancement of high-efficiency CZTS/CdS based solar cells with MoO_x HTL and "Au" bottom contacts.

Statements & Declarations

Funding

The authors declare that no funds, grants, or other support were

received during the preparation of this manuscript.

Author Contributions

The study's conception and design were contributed to by all of the authors. Material preparation, data collecting, and analysis were provided and written by Ph. D students Abdelaziz AIT ABDELKADIR and Professor Mustapha SAHAL. All of the writers read and approved the final paper.

Research Data Policy and Data Availability Statements

The datasets generated and analyzed during the current study are available from the corresponding author on reasonable request.

All data generated and analyzed in this original work research are included in this published paper as tables, figures, and detailed parameters with their reference's sources.

Declaration of Competing Interest

The authors declare that they have no known competing financial interests or personal relationships that could have appeared to influence the work reported in this paper.

Data availability

Data will be made available on request.

Acknowledgments

The authors acknowledge Dr. Marc Burgelman of the University of Ghent in Belgium for providing the SCAPS 1D simulation program, as well as everyone who contributed to this scientific work.

References

[1] L. Sravani, S. Routray, M. Courel, K.P. Pradhan, Loss mechanisms in CZTS and CZTSe Kesterite thin-film solar cells: Understanding the complexity of defect density, Sol. Energy 227 (2021) 56–66.
[2] H. Katagiri, K. Jimbo, W.S. Maw, K. Oishi, M. Yamazaki, H. Araki, A. Takeuchi, Development of CZTS-based thin film solar cells, Thin Solid Films 517 (2009) 2455–2460.
[3] M. Ravindiran, C. Praveenkumar, Status review and the future prospects of CZTS based solar cell–A novel approach on the device structure and material modeling for CZTS based photovoltaic device, Renew. Sustain. Energy Rev. 94 (2018) 317–329.
[4] H. Matsushita, T. Ichikawa, A. Katsui, Structural, thermodynamical and optical properties of Cu2-II-IV-VI4 quaternary compounds, J. Mater. Sci. 40 (2005) 2003–2005.
[5] H. Katagiri, K. Jimbo, S. Yamada, T. Kamimura, W.S. Maw, T. Fukano, T. Ito, T. Motohiro, Enhanced conversion efficiencies of Cu2ZnSnS4-based thin film solar cells by using preferential etching technique, Appl. Phys Express 1 (2008), 041201.
[6] Z. Yang, Research on one-step Preparation of CZTS films and electrochemical optical properties, Dalian University of Technology, 2011 [MS thesis],.
[7] H. Araki, Y. Kubo, K. Jimbo, W.S. Maw, H. Katagiri, M. Yamazaki, K. Oishi, A. Takeuchi, Preparation of Cu2ZnSnS4 thin films by sulfurization of co-electroplated Cu-Zn-Sn precursors, Phys. Status Solidi C 6 (2009) 1266–1268.
[8] W. Shockley, H.J. Queisser, Detailed balance limit of efficiency of p-n junction solar cells, J. Appl. Phys. 32 (1961) 510–519.
[9] W. Wang, M.T. Winkler, O. Gunawan, T. Gokmen, T.K. Todorov, Y. Zhu, D.B. Mitzi, Device characteristics of CZTSSe thin-film solar cells with 12.6% efficiency, Adv. Energy Mater. 4 (2014) 1301465.
[10] B. Shin, O. Gunawan, Y. Zhu, N.A. Bojarczuk, S.J. Chey, S. Guha, Thin film solar cell with 8.4% power conversion efficiency using an earth-abundant Cu2ZnSnS4 absorber, Progress in Photovoltaics, Res. Appl. 21 (2013) 72–76.
[11] P. Fan, Z. Xie, G. Liang, M. Ishaq, S. Chen, Z. Zheng, C. Yan, J. Huang, X. Hao, Y. Zhang, Z. Su, High-efficiency ultra-thin Cu2ZnSnS4 solar cells by double-pressure sputtering with spark plasma sintered quaternary target, Journal of Energy, Chemistry 61 (2021) 186–194, https://doi.org/10.1016/j.jechem.2021.01.026.
[12] P. Fan, J. Lin, J. Hu, Z. Yu, Y. Zhao, S. Chen, Z. Zheng, J. Luo, G. Liang, Z. Su, Over 10% Efficient Cu2CdSnS4 Solar Cells Fabricated from Optimized Sulfurization, Adv. Funct. Mater. 32 (2022) 2207470, https://doi.org/10.1002/adfm.202207470.
[13] X.-Y. Chen, M. Ishaq, N. Ahmad, R. Tang, Z.-H. Zheng, J.-G. Hu, Z.-H. Su, P. Fan, G.-X. Liang, S. Chen, Ag, Ti dual-cation substitution in Cu2ZnSn(S, Se)4 induced growth promotion and defect suppression for high-efficiency solar cells, J. Mater. Chem. A. 10 (2022) 22791–22802, https://doi.org/10.1039/D2TA05909F.
[14] Z. Su, G. Liang, P. Fan, J. Luo, Z. Zheng, Z. Xie, W. Wang, S. Chen, J. Hu, Y. Wei, Device postannealing enabling over 12% efficient solution-processed Cu2ZnSnS4 solar cells with Cd2+ substitution, Adv. Mater. 32 (2020) 2000121.
[15] A. Polizzotti, I.L. Repins, R. Noufi, S.-H. Wei, D.B. Mitzi, The state and future prospects of kesterite photovoltaics, Energ. Environ. Sci. 6 (2013) 3171–3182.
[16] X. Liu, Y. Feng, H. Cui, F. Liu, X. Hao, G. Conibeer, D.B. Mitzi, M. Green, The current status and future prospects of kesterite solar cells: a brief review, Prog. Photovolt. Res. Appl. 24 (2016) 879–898.
[17] Y. Zhao, Z. Yu, J. Hu, Z. Zheng, H. Ma, K. Sun, X. Hao, G. Liang, P. Fan, X. Zhang, Z. Su, Over 12% efficient kesterite solar cell via back interface engineering, J. Energy Chem. 75 (2022) 321–329, https://doi.org/10.1016/j.jechem.2022.08.031.
[18] S.N.S. Nishiwaki, N.K.N. Kohara, T.N.T. Negami, T.W.T. Wada, MoSe 2 layer formation at Cu (In, Ga) Se 2/Mo Interfaces in High Efficiency Cu (In1-xGa x) Se 2 Solar Cells, Jpn. J. Appl. Phys. 37 (1998) L71.
[19] T. Kato, H. Hiroi, N. Sakai, H. Sugimoto, Buffer/absorber interface study on Cu2ZnSnS4 and Cu2ZnSnSe4 based solar cells: band alignment and its impact on the solar cell performance, in: 28th European Photovoltaic Solar Energy Conference, 2013: pp. 2125–2127.
[20] S. Enayati Maklavani, S. Mohammadnejad, The impact of the carrier concentration and recombination current on the p+ pn CZTS thin film solar cells, Opt. Quant. Electron. 52 (2020) 1–23.
[21] J. Liu, W. Chen, X. Feng, Numerical simulation of ultra-thin CdTe solar cells with a buffer layer of MoOx in the backwall configuration, Chin. J. Phys. 56 (2018) 1826–1833.
[22] M.N. Tousif, S. Mohammad, A.A. Ferdous, A. Hoque, Investigation of different materials as buffer layer in CZTS solar cells using SCAPS, J. Clean Energy Technol. 6 (2018) 293–296.
[23] A. Srivastava, P. Dua, T.R. Lenka, S.K. Tripathy, Numerical simulations on CZTS/CZTSe based solar cell with ZnSe as an alternative buffer layer using SCAPS-1D, Mater. Today:. Proc. 43 (2021) 3735–3739.
[24] T.P. Dhakal, C.-Y. Peng, R.R. Tobias, R. Dasharathy, C.R. Westgate, Characterization of a CZTS thin film solar cell grown by sputtering method, Sol. Energy 100 (2014) 23–30.
[25] E. Oublal, A. Ait Abdelkadir, M. Sahal, High performance of a new solar cell based on carbon nanotubes with CBTS compound as BSF using SCAPS-1D software, J. Nanopart. Res. 24 (2022) 202.
[26] A. Houimi, S.Y. Gezgin, B. Mercimek, H.Ş. Kılıç, Numerical analysis of CZTS/n-Si solar cells using SCAPS-1D. A comparative study between experimental and calculated outputs, Opt. Mater. 121 (2021), 111544, https://doi.org/10.1016/j.optmat.2021.111544.
[27] E.K. Chiew, M. Yahaya, A.P. Othman, Investigation of Recombination Process of P3HT: PCBM Organic Solar Cell, Adv. Mat. Res. 622–623 (2013) 1147–1151, https://doi.org/10.4028/www.scientific.net/AMR.622-623.1147.
[28] A.A. Abdelkadir, E. Oublal, M. Sahal, A. Gibaud, Numerical simulation and optimization of n-Al-ZnO/n-CdS/p-CZTSe/p-NiO (HTL)/Mo solar cell System using SCAPS-1D, Results in Optics. (2022), 100257.
[29] A.A. Abdelkadir, M. Sahal, E. Oublal, N. Kumar, A. Benami, Performance enhancement investigations of the novel CZTGS thin-film solar cells, Opt. Mater. 133 (2022), 112969, https://doi.org/10.1016/j.optmat.2022.112969.
[30] S. Chen, A. Walsh, X.-G. Gong, S.-H. Wei, Classification of lattice defects in the kesterite Cu2ZnSnS4 and Cu2ZnSnSe4 earth-abundant solar cell absorbers, Adv. Mater. 25 (2013) 1522–1539.
[31] K. Diwate, K. Mohite, M. Shinde, S. Rondiya, A. Pawbake, A. Date, H. Pathan, S. Jadkar, Synthesis and characterization of chemical spray pyrolysed CZTS thin films for solar cell applications, Energy Procedia 110 (2017) 180–187.
[32] O. Gunawan, T.K. Todorov, D.B. Mitzi, Loss mechanisms in hydrazine-processed Cu 2 ZnSn (Se, S) 4 solar cells, Appl. Phys. Lett. 97 (2010), 233506.
[33] A. Ait Abdelkadir, M. Sahal, E. Oublal, N. Kumar, A. Benami, New Sb2Se3-based solar cell for achieving high efficiency theoretical modeling, Opt Quant Electron. 55 (2023) 514, https://doi.org/10.1007/s11082-023-04797-7.
[34] A. Ait Abdelkadir, E. Oublal, M. Sahal, B.M. Soucase, A. Kotri, M. Hangoure, N. Kumar, Numerical Simulation and Optimization of n-Al-ZnO/n-CdS/p-CIGS/p-Si/p-MoOx/Mo Tandem Solar Cell, Silicon. (2022) 1–11.
[35] B. Liu, J. Guo, R. Hao, L. Wang, K. Gu, S. Sun, A. Aierken, Effect of Na doping on the performance and the band alignment of CZTS/CdS thin film solar cell, Sol. Energy 201 (2020) 219–226.
[36] Y.F. Tay, S.S. Hadke, M. Zhang, N. Lim, S.Y. Chiam, L.H. Wong, Improving the interfacial properties of CZTS photocathodes by Ag substitution, J. Mater. Chem. A 8 (2020) 8862–8867.
[37] S. Lie, J.M.R. Tan, W. Li, S.W. Leow, Y.F. Tay, D.M. Bishop, O. Gunawan, L. H. Wong, Reducing the interfacial defect density of CZTSSe solar cells by Mn substitution, J. Mater. Chem. A 6 (2018) 1540–1550.
[38] Y. Zhang, K. Tse, X. Xiao, J. Zhu, Controlling defects and secondary phases of CZTS by surfactant potassium, Phys. Rev. Mater. 1 (2017), 045403.
[39] F. Liu, J. Huang, K. Sun, C. Yan, Y. Shen, J. Park, A. Pu, F. Zhou, X. Liu, J.A. Stride, Beyond 8% ultrathin kesterite Cu2ZnSnS4 solar cells by interface reaction route controlling and self-organized nanopattern at the back contact, NPG Asia Mater. 9 (2017) e401–e.
[40] O.K. Simya, A. Mahaboobbatcha, K. Balachander, A comparative study on the performance of Kesterite based thin film solar cells using SCAPS simulation program, Superlattice. Microst. 82 (2015) 248–261.